Phytochemical assisted synthesis of Ni doped ZnO nanoparticles using aloe vera extract for enhanced photocatalytic and antibacterial activities

K. L. Mary[a,b], J. V. Manonmoni[a*], A. M. R. Balan[c], P. S. Karthik[d], S. P. Malliappan[e]
[a]*Department of Chemistry, Annamalai University, Chidambaram, India.600802*
[b]*Department of Chemistry, IFET College of Engineering, Gangarampalayam, 605602.*
[c]*Department of Chemistry, Jawaharlal Nehru College for women, Ulundurpet, 606104.*
[d]*Department of Chemistry, University College of Engineering, Panruti-607106.*
[e]*Sunum, Sabanci University, University Cd.No:27, Istanbul, Turkey.*

This report focuses on facile and green approach to synthesize ZnO and Ni doped ZnO nanoparticls (NPs) through a phytochemical assisted method using an aloe vera extract as reducing and capping agent. The phase confirmation, structural morphology, surface area, chemical compositions of as prepared NPs were investigated in depth using several techniques such as XRD, FTIR, UV-Vis, SEM, TEM, PL and XPS techniques. The photo catalytic activity of the NPs evaluated towards the degradation of two toxic dyes such as Crystal violet(CV) and Congo red (CR). The antimicrobial activity of the NPs evaluated against E.Coli, Klbsiella Pneumoniae, Staphylococcus aureus and Streptococcus pyogenes. As a result of conducted experiments, it was found that Ni-doped ZnO exhibits better photocatalytic and antibacterial activities compared to pristine ZnONps. The mechanism of enhanced activities discussed in detail.

(Received February 15, 2022; Accepted May 25, 2022)

Keywords: Ni doped ZnO, Aloe vera extract, Photo catalytic activity, Antibacterial activity

1. Introduction

The accumulation of huge contaminants generated from food and textile industries in water has caused the severe environmental problems and creates severe impact on human health issue [1-3]. Since photo catalytic materials have great potential applications for decomposing contaminants and killing bacteria in the environment, is an effective strategy to solve environmental challenges [4-5]. In the past decades, research and development in nanotechnology has gained considerable attention owing to their unique features and wide range of applications especially in pharmaceuticals as well as antibacterial, antimicrobial and cytotoxicity effects [6-7]. Nanotechnology can be used in nano medicine to discover and develop new materials for antibacterial properties; its impacts extend from medical filed into environmental field.

As a result of development of nanotechnology, metal oxide nanoparticles emerged as interesting materials for treatment of antimicrobial disease, cancer and cleaning water [8-9]. Among the various metal oxides, ZnO is gaining attention by researchers owing to its applications in the field of biomedical as well as in environment. ZnO is most valuable nanomaterial and is potential to be used in medical applications owing to its excellent properties of low toxicity, biocompatibility and biodegradability [10]. Since Zinc is an essential trace element extensively exists in all body tissues and takes part in body's metabolism, plays a crucial in biomedical applications such as anticancer, drug delivery, antibacterial, anti-inflammation etc. [11-13].

Although ZnO nanoparticles widely used in medical field, one of the drawbacks is, it presents toxic effect on human animal cells. Potential toxic effects of ZnO nanoparticles on

* Corresponding author: vijilalovelin@gmail.com
https://doi.org/10.15251/DJNB.2022.172.634

various cell lines are reported in literature [14-15]. In general, the toxicity contributed by chemical reaction during the chemical synthesis limits its potential biological application [16]. Additionally, chemical reagents used in chemical synthesis are hazardous to the environment.

Thus, to overcome these complications, the principle of green chemistry utilizing natural origin sources plants, leaves, flowers, seeds, fruit peels, roots, microbes for the synthesis process may prove to be a potential solution [17]. Plants could be widely used due to their abundance, easy availability and environment compatibility without inducing adverse environmental impacts. Based on the literature reports, ZnO nanoparticles have been synthesised by various plant extracts such as Satureja hortensis [18], Cuminum cyminum [19], Hibiscus sabdariffa [20] and Acalypha indica leaves [21], Cochlospermumreligiosum[22], Tabernaemontanadivaricata [23] and Conyza Canadensis, Citrus maxima [24] and their biological properties were also reported.

Aloe Barbadensis Miller (Aloe vera) is a cactus -like plant since it is succulent, covered with wax and contains over 75 active compounds such as vitamins, enzymes, phenols, acids etc. [25]. It has been reported to possess antibacterial, anti-inflammatory, wound-healing, anti-diabetic properties and discovered it can be a benefit in medicinal filed particularly for cancer treatment [26]. Since the peel extract contains reducing agent, which can be used to synthesise nanoparticles with good crystalline structure [27]. Keeping in view the importance of Aloe vera in medicine and due to their low cost, environmentally friendly nature coupled with their reducing properties we selected aloe vera as reducing and stabilizing agent to prepare ZnO nanoparticles.

Based on considering the medical importance aloe vera as well as zinc oxide, we hereby report an eco-friendly approach for the synthesis of zinc oxide nanoparticles using aloe vera extract as a reducing agent and we found the phytochemicals present in aloe vera promotes the formation of nanoparticles as well as control the size of the particles. To enhance the UV absorption and photo catalytic efficiency of Zinc oxide, it is doped with the transition element Ni which could enhance its optical and other properties. The synthesized zinc oxide nanoparticles were investigated for photo catalytic, antibacterial properties. To the best of our knowledge this is the first report about the photo catalytic, antibacterial activities of Ni doped ZnO nanoparticles synthesised by aloe vera extract.

2. Materials and methods

2.1. Materials

For the Zinc oxide nanoparticles synthesis, the following Sigma-Aldrich made materials were used without further purifications. All the solutions were prepared with deionized water. Aloe vera leaves, Zinc acetate dihydrate, ($Zn(OAc)_2.2H_2O$), Nickel chloride dihydrate ($NiCl_2.2H_2O$) and Sodium hydroxide were used were used as reducing agent, zinc precursor, Nickel source, synthesis medium respectively.

2.2. Preparation of Aloe vera leaf extract

Fresh and healthy leaves of Aloe Vera plant were collected locally then washed thoroughly with fresh water and the internal mucilaginous was used for extract preparation. 50 g of fresh gel was crushed with the help of pestle, mortar and added to 100 ml of distilled water. The slurry was stirred and placed in water bath at 70^0C for one hour. Afterward, it was filtered by No.1 Whatman filter paper. As a result, pale green colored solution of filtrate was collected and stored in refrigerator for further investigations.

2.3. Synthesis of Ni doped ZnO Nanoparticles

The ZnO NPs are synthesized by eco-friendly plant extract assisted green method. In a typical synthesis, 100 ml of 0.01 N of Zinc precursor solutions was mixed with few drops of Sodium hydroxide solution; addition was continued until the pH level reached about 10. The mixture was vigorously stirred for half an hour for completion of reaction between the zinc acetate and sodium hydroxide. Then 50 ml of plant extract solution was added to the reaction mixture and magnetically stirred for 30 minutes. This reaction mixture was heated to 60^0C for 3 hours with occasional stirring. This led to the change of color from grey to white and appeared as creamy

paste, which confirms the formation of biologically reduced ZnO nanoparticles. The white precipitate obtained was filtered and washed thrice with solvent to ensure the removal of impurities. Finally, the dried sample was calcinated for lyophilization in a muffle furnace at 400^0C for 2 h. Lyophilized ZnO nanoparticles were stored in cool, dry place and further characterization was carried out. For the preparation of pure ZnO, the same procedure was followed without Ni sources. The synthesis scheme is illustrated in Fig.1.

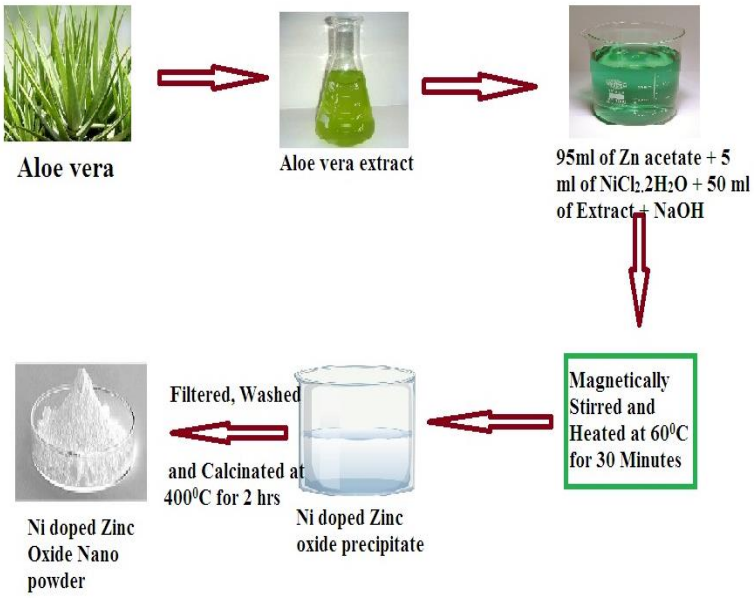

Fig. 1. Schematic illustration of synthesis process.

2.4. Photo catalytic measurement

Photo catalytic activity of ZnO and Ni doped nanoparticles were investigated by observing the degradation of Congo red and Crystal violet dyes under day light irradiation. In these experiments, 5 mg of photo catalyst was placed in 40 ml of dye solution (0.025 gml^{-1}). This solution was stirred for 15 minutes in the absence of light to reach adsorption-desorption equilibrium before illumination. Then the solution was continuously stirred for 2 hours under visible light irradiation (λ>400 nm). At 15 minutes time intervals, 5 ml simple was withdrawn and centrifuged to remove the catalyst. The concentration of the supernatant in each sample was analyzed using UV-Visible spectrophotometer at the characteristic wavelength of dyes (498 nm and 588 nm for MO and CV respectively). In addition, blank experiments were also performed under the same condition without the catalyst to investigate the degradation efficiency of the catalyst.

2.5. Antibacterial activity of ZnO NPs

The antibacterial activity of as synthesized ZnO nanoparticles was investigated by well diffusion method (28) with different species of pathogens such as E.Coli, Klbsiella Pneumoniae, Staphylococcus aureus, and Streptococcus pyogenes. The nutrient agar was served as medium for bacterial growth which was poured into the sterilized petriplates and allowed for solidify. The tested bacteria were spread evenly on nutrient agar plates using a sterile loop. Six wells of 6 mm diameter were made on MH agar plate using sterilized pipette. These wells were filled then with 50 µL solution containing ZnO nanoparticles of various concentrations such as 8, 16, 40 mg/ml. Control wells were filled with 50 µL of distilled water. The samples were initially incubated for 15 minutes at 4^0C (to allow diffusion) and later at 37^0C for 24h. After the incubation, the formation of zone around the well was observed to determine the sensitivity of each antibiotic. The inhibition zone around the discs was measured by digital micrometer. The greater the diameter of the inhibitory zone, the greater antimicrobial activities of nanoparticles.

2.6. Characterization

X-ray diffraction experiments were performed by Rigaku Ultima III X-ray Diffract meter using Cu Ka radiation (k = 1.54 A˚) in the 2h range from 20 to 80.FTIR spectra of the samples were analyzed by JASCO-460 plus spectrometer operated at 4 cm−1 resolutions in the range of 400-4000 cm−1.The UV–VIS absorption spectrum was recorded on a Perkin- Elmer lambda 950 UV–vis.–NIR spectrophotometer. The surface morphology and roughness of ZnO NWLs were performed usingg high resolution transmission electron microscope (FEI Tecnai T 20 U-Twin TEM) with the accelerating voltage of 200 kV. The surface electronic states of the samples were analyzed by X-ray photoelectron spectroscopy (XPS, AXIS Ultra DLD (Kratos.Inc), Monochromatic Al Ka radiation (1486.6 eV, 150 W). Photoluminescence (PL) measurements were carried out at room temperature at an excitation wavelength of 325nm. The specific surface areas and porous nature of materials were further investigated by nitrogen adsorption/desorption measurements on nova 2200e.

3. Result and discussion

3.1. Powder X-ray Diffraction Analysis

Phase identification and crystallite size of the sample were investigated by X-ray diffractometer. The XRD pattern of as prepared ZnO and Ni doped ZnO nano structure is shown in Fig.2. It can be observed from figure that the diffraction 31.79°, 33.43°, 36.24°, 47.65°, 56.71°, 62.96°, 68.24°, and 69.20° have been indexed as hexagonal wurtzite phase of ZnO [29] with lattice constants JCPDS No. 36-1451, a = 3.2987 Å,c = 5.2921 Å).The diffraction peak corresponding to the plane of (101) become more evidenced. There was no additional peak for Ni doped Zn which confirms the high purity and crystallinity of the doped samples. The absence of peaks corresponding to Ni ion in the XRD pattern indicates that the wurtzite structure is unaltered by the addition of Ni-ions.

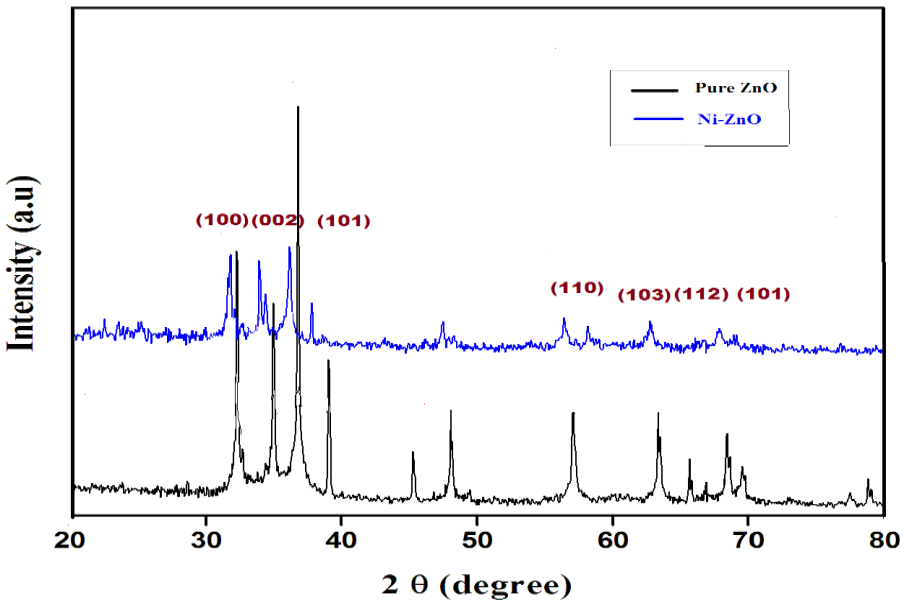

Fig. 2. Powder XRD pattern of ZnO and Ni doped ZnO.

The increase in intensity of the peak and decrease in FWHM of the particular diffraction peak were observed for Ni doped sample which clearly indicates the successful incorporation of Ni in the ZnO matrix, which can be attributed to the difference of ion radius of Zn^{2+} (0.74 Å)

comparing with that of Ni^{2+} (0.74 Å). Moreover, higher angle shift for the diffraction peak of (100) were observed for Ni doped sample.

The mean crystallite size and lattice parameters of the prepared sample Lattice parameter were calculated by Debye–Scherrer formula [30] and by well-known analytical method [31] and listed in Table 1. The average crystallite size was found to be 26nm and 19nm for pure and Ni doped ZnO respectively. The calculated crystallite size is found to be decreased with Ni doping. This might be due to the incorporation of Ni in ZnO matrix which has decrease the nucleation of the particle as well as the growth of crystallites.

Table 1. Structural parameters of ZnO and Co-doped ZnO samples at room temperature obtained from Rietveld refinement.

Samples	Crystallite size (nm)	a(Å)	b(Å)	c(Å)
Pure ZnO	26	3.2987	3.2927	5.2921
Ni ZnO	19	3.2962	3.2962	5.2913

3.2. SEM and TEM Analysis

The size, shape and morphology of the ZnO and Ni doped ZnO were investigated by SEM and TEM analysis. The SEM images of ZnO and Ni doped ZnO are shown in Fig. 3a, b. It was clearly shown that both the samples have well spherical like morphology with average diameter around 20-30 nmwhich indicates that Ni doping has no apparent change in structure of ZnO matrix. Regardlesstheincorporation of Ni ion not altering the structure of ZnO, some pores between the grains were observed for doped ZnO.

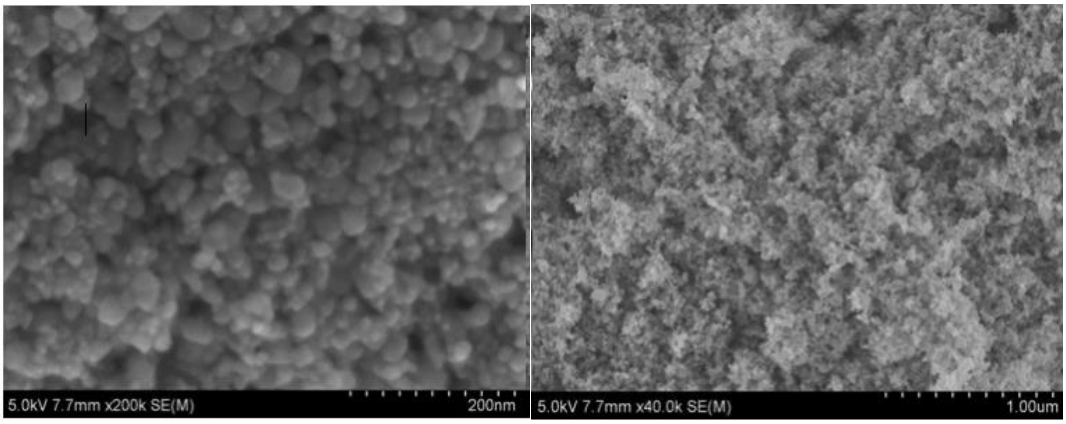

Fig.3 SEM images of a) ZnO and b) Ni doped ZnO

The TEM images of ZnO and Ni doped ZnO are shown in Fig. 4a, b. It was clearly demonstrates the formation of microspheres with largely uniform sphere and with well-defined structure. The uniform sphere formation strongly revealed that the phytochemicals in aloe vera extract has effectively influenced on the morphology and size of ZnO nanostructures and hence this synthesis process effectively generated samples. The chemical compositions of the Ni-doped ZnO are measured by the energy dispersive X-ray (EDX) spectroscopy analysis and shown in Fig.4. c. It can be seen that the samples existence with the major element such as Zn, Ni, Co and O elements without other impurity peaks which confirms that the prepared nanostructure is pure of Ni dopedZnO. Furthermore, the SAED pattern of the ZnO is shown in Fig.4.d, which confirms the crystalline nature of the sample.

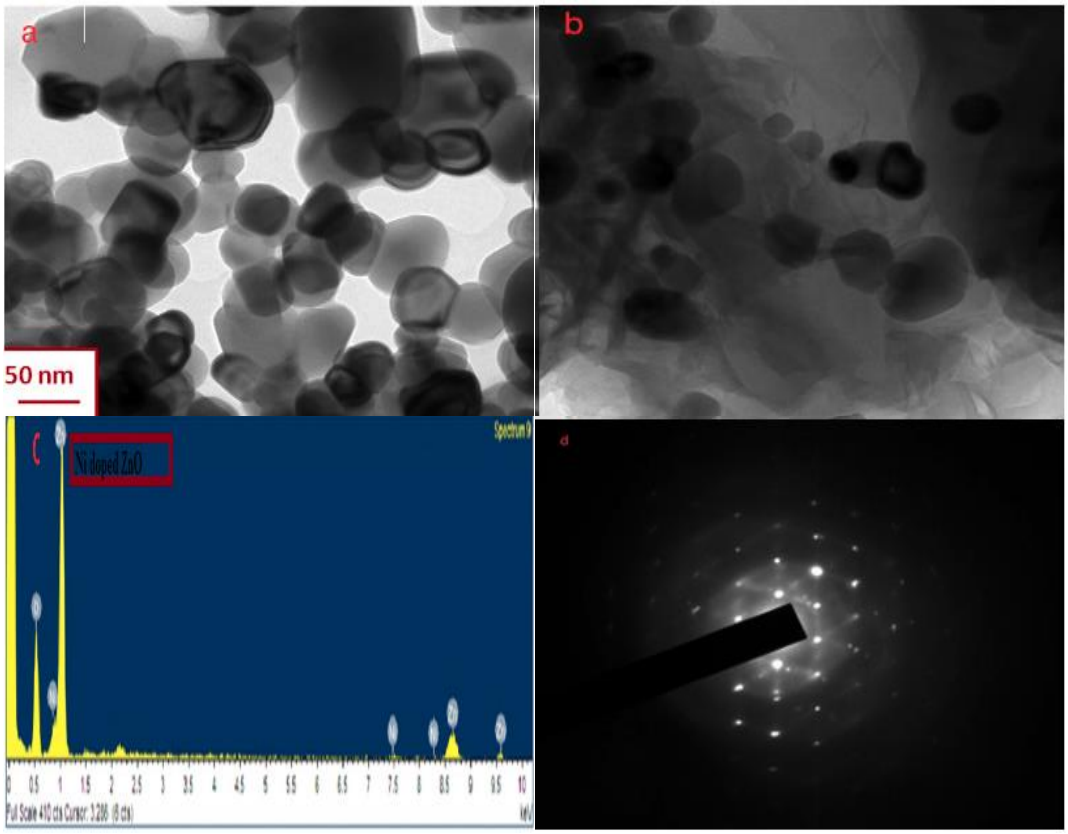

Fig. 4. TEM images of a) ZnO b) Ni doped ZnO C) EDAX spectra of Ni-ZnO d) SAED pattern of ZnO.

3.3. UV-Vis Spectral Analysis

Fig.5.a shows the UV-Vis absorption spectra of ZnO and Ni-ZnO nanoparticles at room temperature. The sharp absorption peak of well-defined exciton band appeared at 370 nm and 363 nm for pure and Ni doped ZnO respectively which is due to the free excitons of ZnO nanostructures. The excitonic peaks clearly exhibit blue shift for Ni doped ZnO which might be attributed to surface effecs, modification in size and morphology. In general, absorbance value is dependent on various factors like the size of particles, deformities in grain structure, oxygen deficiency etc. In the absorption of spectra of Ni doped ZnO, there is no absorption peak for Ni ion where it will be appear between 550 nm to 700 nm[32]. This blue shift may be the reason of Burstein-Moss effect [33]. Fig 5.b shows the plot of $(\alpha hv)^2$ versus photon energy hv for ZnO and Ni doped ZnO. Linearity of the plot reveals that both the materials are direct transition type semiconductors. The band gap energy (Eg) values for pure and Ni-doped ZnO nanoparticles were obtained by extrapolating to $(\alpha hv)^2 = 0$ and it was found to be 3.29 eV and 3.25eV respectively. There is significant reduction in ban d gap energy was noted for Ni doped ZnO compared to pure ZnO nanostructure and this is due to the charge transfer between the Ni^{2+} ions and Zn^{2+} ions in their CB or VB band level. It can be inferred from the reducing band gap that Ni^{2+} ion have been homogeneously included in Zn site of ZnO lattice. The reduction in band gap energy in Ni doped ZnO have been expected to demonstrate improved photo catalytic and antibacterial properties in it.

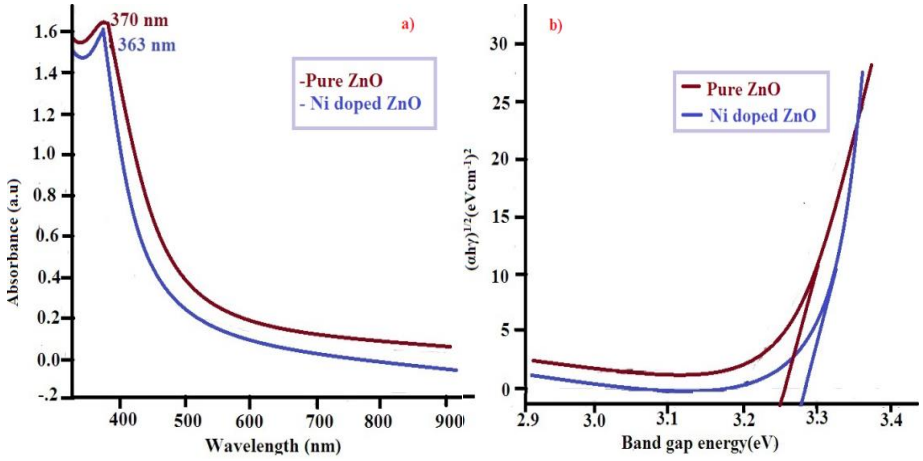

Fig. 5. a)UV-Vis spectra of ZnO and Ni doped ZnO b) Band gap energy calculation.

3.4. Photoluminescence Spectral Analysis

PL spectral investigation is significant method to identify the luminescence behaviour and the recombination rate of photo generated electron-hole pairs. PL measurements were performed for pure and Ni doped ZnO samples with excitation wavelength 330 nm and the results are depicted in Fig.6. It can be clearly observed that sharp PL emission peak for centered around 376 nm for pure ZnO samples which is corresponds to near band ultra violet emission. The UV-emission peak was ascribed by near band edge emission transition of ZnO nanomatrix. On the other hand, the intensity of the UV emission peak was totally supressed for Ni-doped ZnO. This might be attributed due to the presence of trap centers, quenching effect and mobility of charge carriers. During the doping, efficient interfacial charge transfer from ZnO shell to Ni core, acting as an electron sink that hampers the recombination of photo-induced carriers [34].

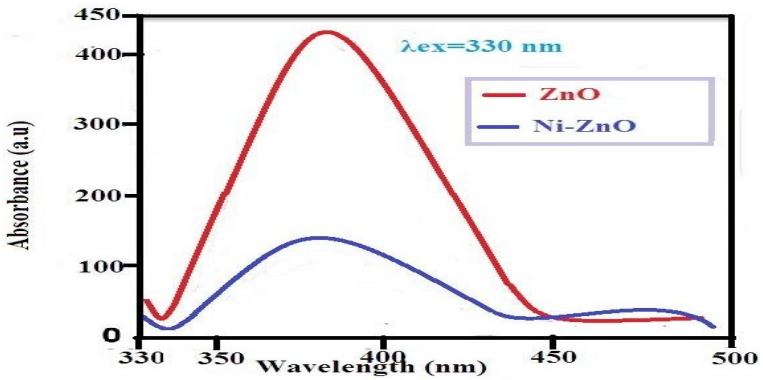

Fig. 6. Photoluminescence spectra of ZnO and Ni doped ZnO.

3.5. FTIR Analysis

The FTIR spectra of sample are used to investigate the structural nature and the chemical composition of as synthesized pure ZnO. FTIR of ZnO was recorded in the range of 400-4000cm^{-1}and shown in Fig.7. In this spectrum, the different bands were observed at 3427 cm $^{-1}$, 2957 cm $^{-1}$, 1459 cm $^{-1}$, 457 cm $^{-1}$. The characteristic clear and broad band obtained around 3427 cm^{-1} is assigned to OH stretching mode of vibration [35]. The peak in the region around 457 cm^{-1}, 1637 cm^{-1} is assigned to Zn-O stretching and deformation vibration respectively [36] which confirms the formation of ZnO nanoparticles using aloe vera extract as capping and reducing agent. Peaks from 1460–1410 cm−1 suggested C-C stretching vibration of alcohol, carboxylic acid, and bands at 946–769 cm−1 demonstrated presence of carboxylic acid and aromatic C-H bending. It is revealed

from the FTIR spectra that in fact, the phytochemicals such as carboxylic acid, ester, proteins and flavonoids molecules present in the leaf extract possibly cause the reduction of metal ions which is in agreement with the previous reports [37].

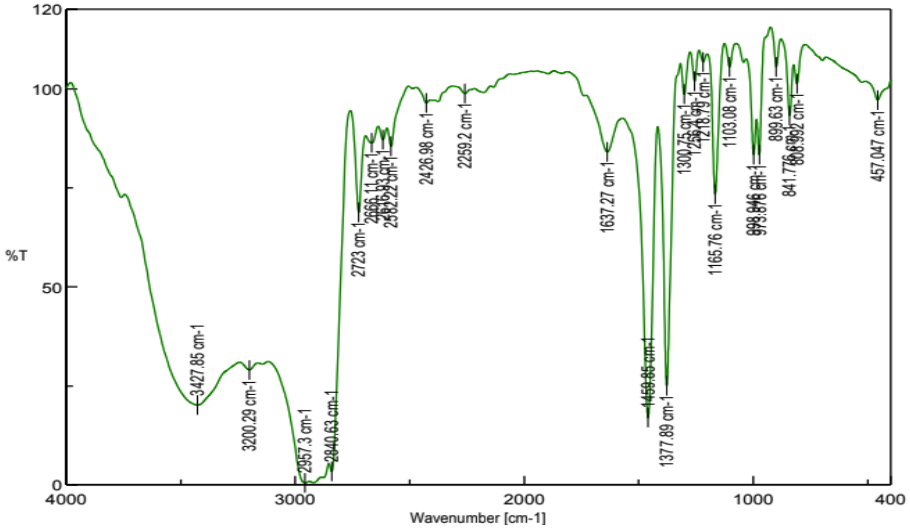

Fig. 7. Infra-red spectra of ZnO.

3.6. XPS Analysis

The elemental composition and oxidation state of as synthesized sample further confirmed by XPS analysis. Fig. 8. represents the low-resolution full range XPS spectra of pure ZnO. The full survey spectrum demonstrates that the consistence of the main element such as Zn and O in the nanostructure. The core level high resolution Zn-2p scanning spectrum exhibits two characteristic peaks with B.E. values of 1015.1 eV and 1024.2 eV which can be assigned for 2p ½ and 2p 3/2 orbitals of Zn respectively.

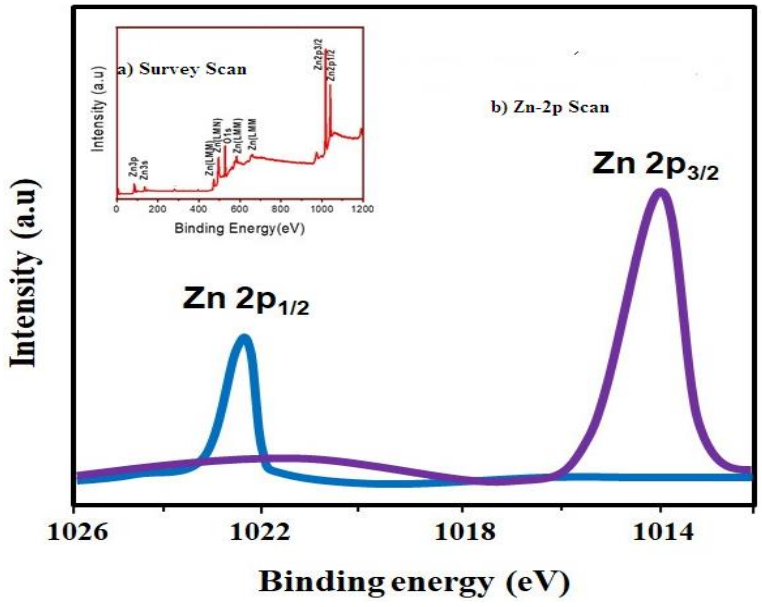

Fig. 8. a) Survey scan spectra and b) Zn-2p scan spectra.

3.7. N_2 adsorption-desorption Analysis

Pore size and surface are are playing a crucial role in enhancing the photo catalytic activities of the catalyst. Hence, N2 adsorption-desorption measurement was adapted to finding the surface area and pore size of as prepared samples and the results are shown in Fig.9.

Figure 9 shows BET surface area of both samples curves which indicates that IV type isotherm and H3 hysteresis loop concurring to standard IUPAC categorization. This is clearly demonstrates that mesoporous nature of the samples [38].The BET surface are of the samples are calculated as 34.1 m^2/g and 85.8 m^2/g for pure and Ni doped ZnO respectively. Additionally, the identical pore size of catalyst calculated as 12.19 nm and 27.72 nm.From the results, it was noted that Ni-doped ZnO nanostructure exhibit higher surface area and pore size than compared to that of pure ZnO and hence which may be expected for higher photo catalytic as well as biological activity.

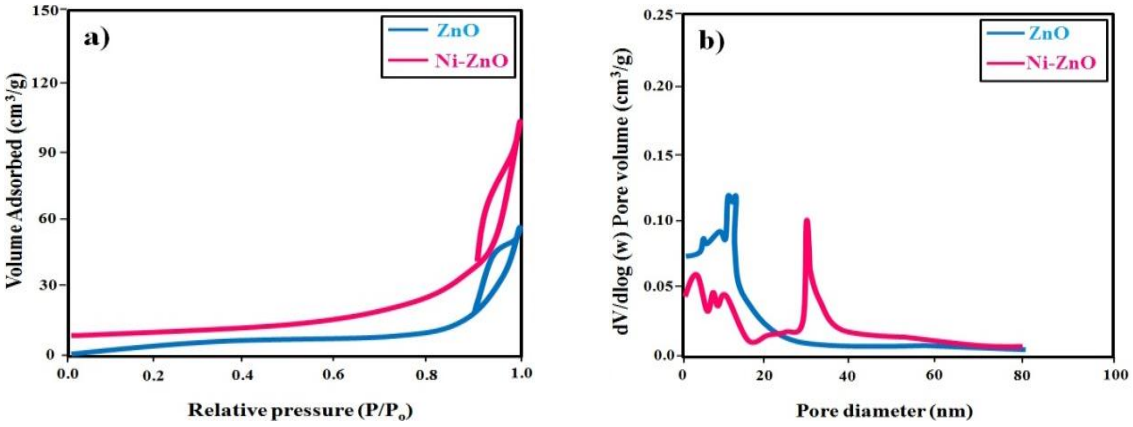

Fig. 9. a) N_2 adsorption spectra and b) pore size distribution of ZnO and Ni doped ZnO.

3.8 Photo catalytic activity

The photo catalytic activity of as synthesized pure ZnO and Ni doped ZnO was analysed for the degradation of two dyes namely Congo Red (CR) and Crystal violet (CV) under irradiation of UV radiation. For the comparison of photo catalytic activity of pure and Ni doped ZnO catalyst, both were evaluated at the same reaction conditions. The degradation of efficiency of catalyst was examined by monitoring their change in concentration with respect to time under UV irradiation. Fig. 10 a & b shows the photo catalytic degradation of CV and CR in presence of Ni doped ZnO catalyst under UV irradiation. From the figure, it was clearly noted, the intensity of characteristic absorption peak (586 nm for CV & 498 nm for CR) decreased with increase of time but there is no shifting of absorption maxima. It can also be seen that the maximum absorption band CV and CR were completely disappeared after 150 minutes. A blank experiment was also performed for the degradation of dyes without catalyst and showed that the concentration of characteristic absorption peak remains unchanged even after 3 hours which confirm that the self-degradation is not possible for dye molecules. The degradation % was also calculated using the formula $(C_0\text{-}(C/C_0)$ X 100, where C_0 is the initial concentration and C is the concentration at different time interval. The photo catalytic efficiency both the catalyst compared at different time interval and the results are given in Fig.11. For Ni doped ZnO, the degradation % of 94.1 and 92.3 were observed at the time of 150 minutes for CV and CR respectively whereas, pure ZnO catalyst shows only the maximum degradation % of 89.3 and 87.1 at the same time. The obtained degradation % is higher and fast compare with previously reported values of ZnO nanostructures [39].

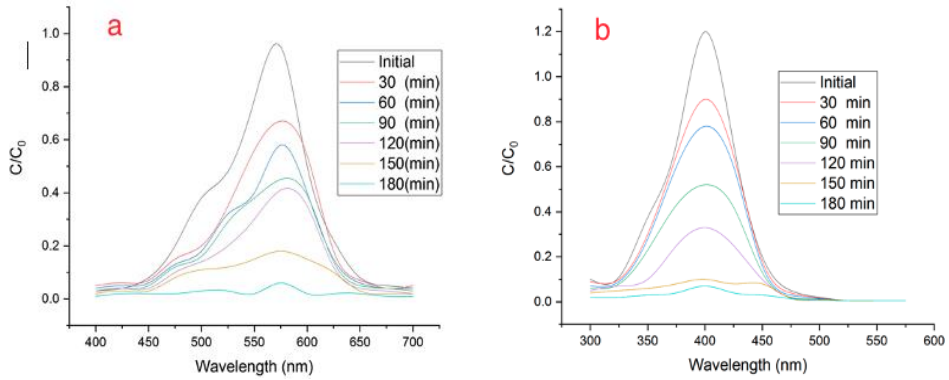

Fig. 10. UV absorption spectra of a) CV and b) CR during photocatalytic degradation by Ni doped ZnO at various time interval.

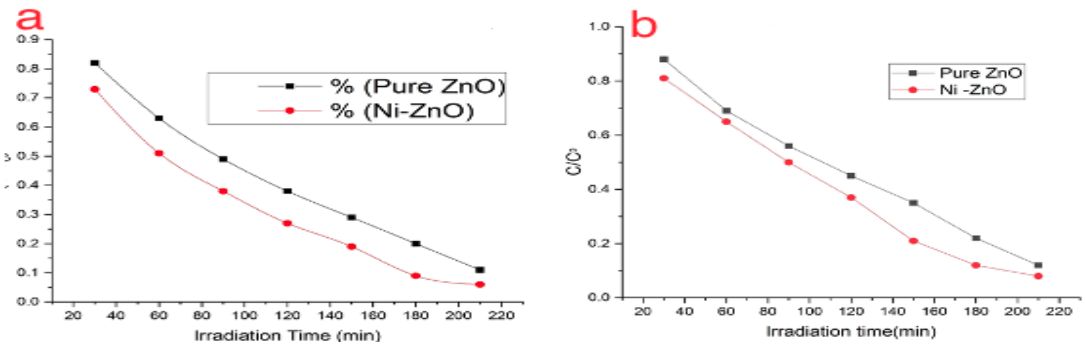

Fig. 11. Percentage of degradation of a) CV and b) CR at various time interval

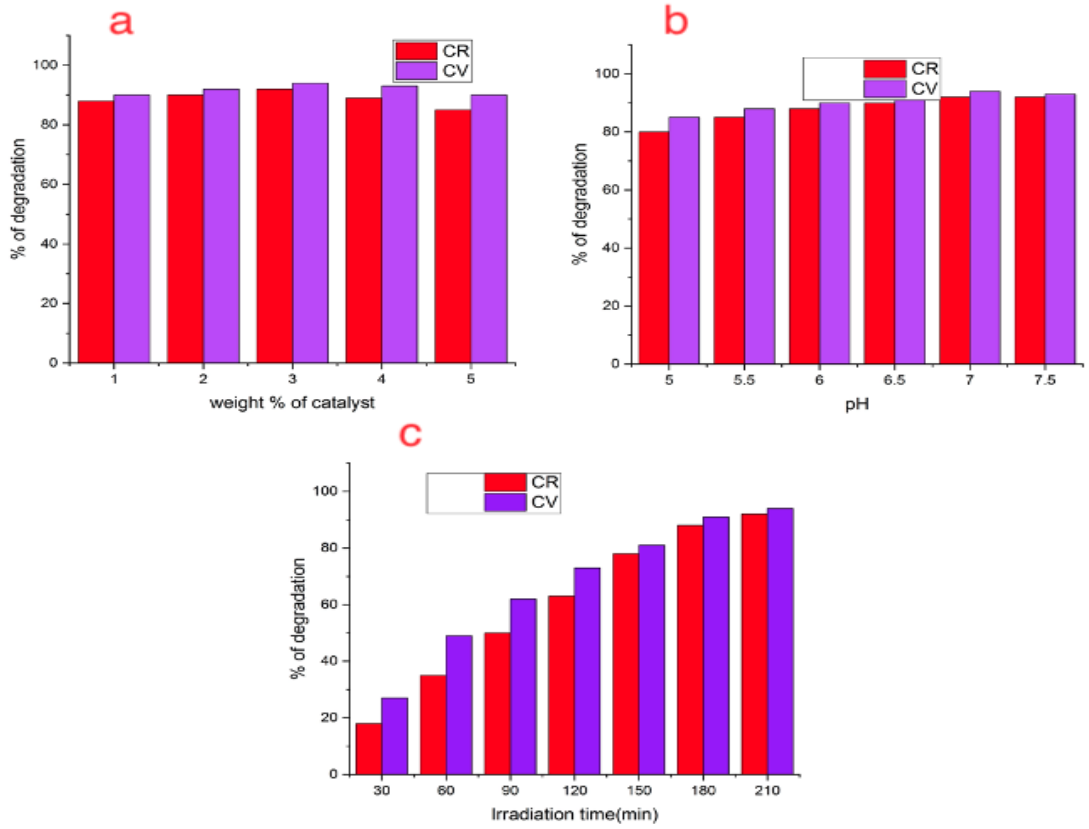

Fig. 12. Effect of a) catalyst dosage b) pH c) irradiation time on photocatalytic degradation of CV.

Further in order to evaluate the effect of catalytic dosage, pH, initial concentration, the degradation experiments were performed for CV dyes at various time, concentration, pH level and the results are depicted in fig.12. It was clearly indicated that the maximum efficiency achieved at 3% weight, pH-6.5 and time-150 minutes and hence optimized concentration, time and pH was fixed as 3% weight, pH-6.5, 150 mins. To study the reaction kinetics of degradation of CV, the experimental data were fitted to first order model as stated by the formula of ln (Co/C) = kt. The reaction rate constant k value can be achieved from the slope of $\ln(C_0/C)$ against time.

Furthermore, to assess reusability and photo stability of the catalyst the cycling test were performed by doing several experiments of degradation of CV using the same catalyst. For this, it was achieved by by collecting the photo catalystwas filtered and dried at 105°C for 24 hours touse for the next cycle. And new photo degradation activity was carried out by utilizing the recovered catalysts. The results of reusability tests of Ni-ZnO are shown in Fig 13. It was clearly depicting there is no loss in its activity up to five runs and only slight variation in removal efficiency was observed after five successive cycles. Ni-ZnO nanostructure exhibits excellent reusability and any remarkable loss of the catalytic activity was not beholden even after six runs and hence it would be a promising material for dye removal.

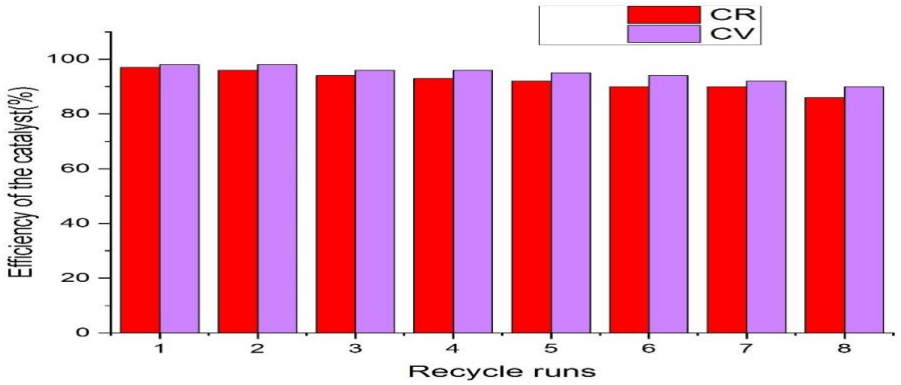

Fig. 13. Reusability test of the Ni-ZnO catalyst.

The plausible mechanism is proposed to explain the enhanced photo catalytic activity of Ni doped ZnO catalyst, based on the photo generation of electron–hole pairs between the conduction and valence band due to excitation of ZnO under UV illumination, as illustrated in Fig. 14. Initially the dye molecule will be adsorbed on the surface of catalyst and then the light energy feed into the system when it is irradiated with UV light, it eject electrons from its valence band (VB) to the conduction band (CB), which promotes the instantaneous creation of the same amount of holes in the VB of ZnO. The photo generated holes and electrons have the most important roles in the degradation of CV and CR which are reacts with environmental oxygen, water molecules tend to form more reactive species such as super oxide anions and hydroxyl radicals. The overallphoto catalytic reactions are as follows [40];

$$ZnO + h\gamma(light) \rightarrow electron(CB) + hole(VB)$$

$$O2 + electron \rightarrow O2-$$

$$2H + +O2 + 2e- \rightarrow H2O2$$

Due to the difference in VB and CB (more negative VB and more positive CB) potential of Ni compared to Zn, the photo induced holes on the valence band and the electrons on the conduction band of ZnO could move to towards Ni.Moreover, the photo catalytic properties of ZnO depend upon various factors like morphology, size, and electronic state and surface area. In general, the nanostructure with smaller size, higher surface area favours the extends of adsorption as well as activates the charge carrier migration [41]. As evident from BET and UV reports, it was

proved that doping of Ni on ZnO has affected on the morphology of nanoparticles, size, surface area and band gap. Ni doping decrease the electron-hole recombination leading to the rapid formation of superoxide radicals and enhanced photo catalytic activity and hence as synthesized Ni doped ZnO nano particles can be used as an efficient photo catalyst for degradation of CV and CR.

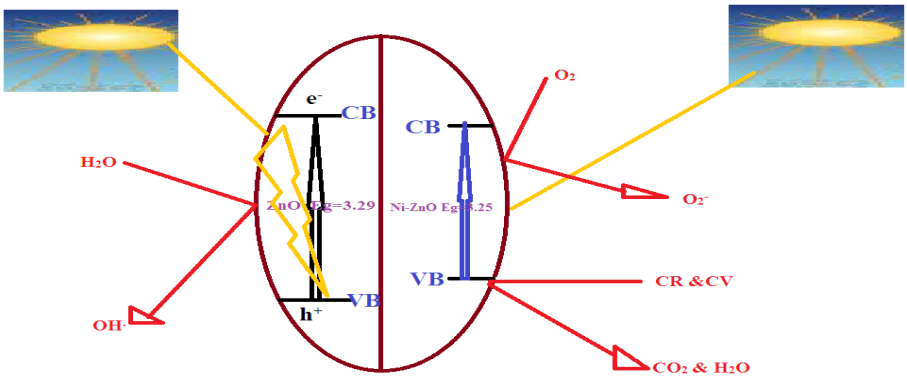

Fig. 14. Photocatalytic mechanism of dye degradation by Ni-ZnO

3.9. Antibacterial activity

Antibacterial activity of green synthesized pure ZnO and Ni doped ZnO were observed by well diffusion method against four different pathogens such as E.Coli, Klbsiella Pneumoniae, Staphylococcus aureus, and Streptococcus pyogenes. The zone of inhibition around the well is shown in Fig. 15. From the figure it is noted that synthesized nanoparticles show significant impact on the growth of bacteria around the well. No inhibition zone was observed for the stack solution taken in well without the nanoparticles. When compared to gram positive bacteria, the higher inhibition zone was observed against gram negative bacteria, which may be ascribed to the difference in cell wall composition of gram-positive and gram-negative bacteria. Moreover, for the all the organism increasing concentration of nanoparticles, growth inhibition of microbes increases. Better antibacterial activity is exhibits at the concentration of 15 µg/ml of stock solution.

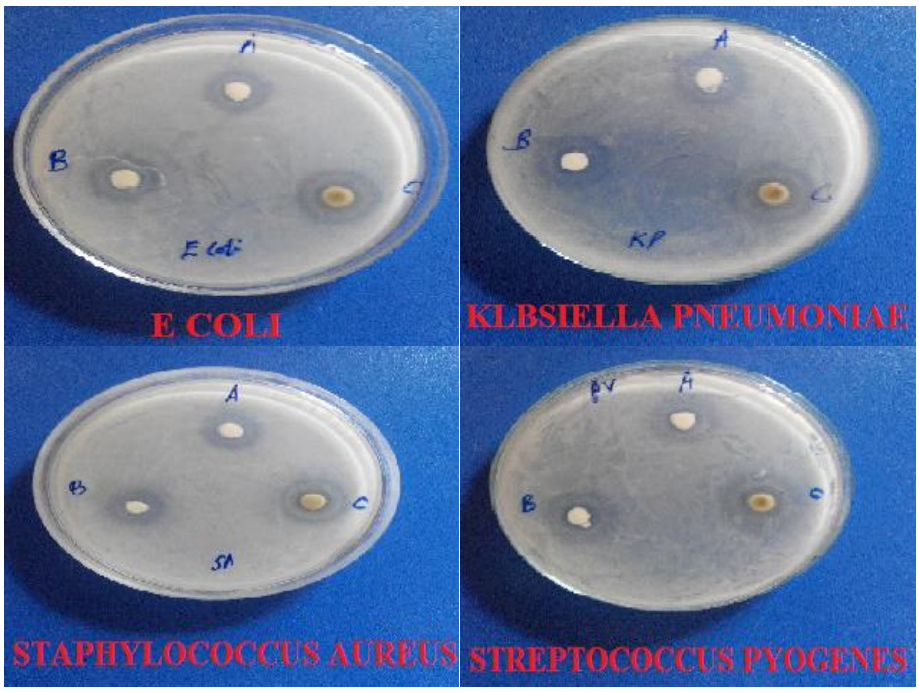

Fig. 15. Antibacterial activity of Ni doped ZnO synthesised by phytochemical method against E coli, Klbsiellapneumor, staphylo coccus, streptococcus.

Further the antibacterial activity of both the particles towards the entire four microorganisms plotted in Fig. 16. Though both the nanoparticles revealed good antibacterial activity against all the bacteria, slightly enhanced antibacterial activities were found for Ni doped ZnO. Among the four, the best inhibition zone was obtained for E. coli bacteria. In general, NPs have greater surface reactivity and easier cell penetration. Release of Zn^{2+} is one of the main reasons for the antibacterial activity of ZnO NPs, which first damage the bacterial cell membrane and then permeates into it. Released ion inhibit several bacterial cell activities including active transport, bacteria metabolism, and enzyme activity leading to bacterial cell death due to the toxicity properties of Zn2+ [42]. The antibacterial activity of ZnO is also due the production of increased levels of ROS, mostly hydroxyl radicals, and singlet oxygen. [43]. It is also established that decreasing the crystallite size by Ni^{2+}-doping increased the surface area, resulting in improved antibacterial activity.[44]. The antibacterial activity of Ni-ZnO nanocatalyst is very significant when compared to that of pure ZnO, which is due to its small size, high surface area and the capability to penetrate easily into the outer cell membrane. The obtained antibacterial activity is higher with previously reported values of ZnO nanostructures [45], which was synthesised by chemical method. This may be due to enriched antibacterial activities of aloe vera.

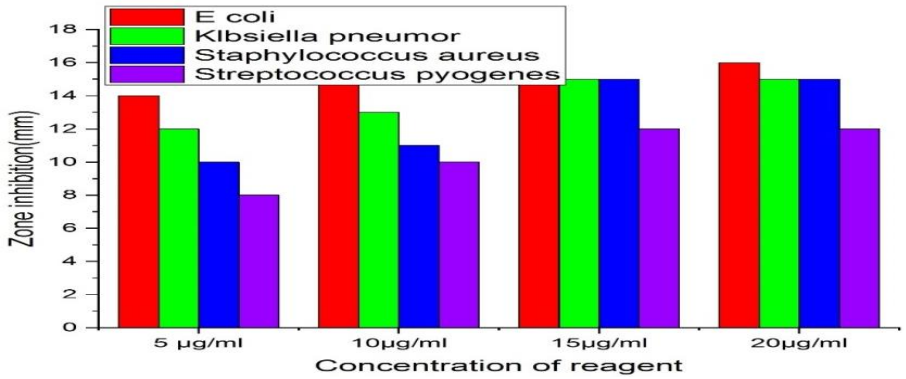

Fig. 16. The antibacterial activity of Ni doped ZnO against E coli, Klbsiellapneumor, staphylo coccus, streptococcus aureus by well diffusion method.

4. Conclusion

In summary, new and cost effective green mediated method is used for the synthesis of pure and Ni doped ZnO using aloe vera leaf extract as the synthesis medium.The characterization studies showed that the samples were in hexagonal wurtzite structure without any impurities and had porous structured morphology. The synthesized ZnO-NPs were alsoeffective in the degradation of CR and CV dyes. Ni doped ZnO, the degradation % of 94.1 and 92.3 were observed at the time of 180 minutes for CV and CR respectively. Thephoto catalytic efficiency of ZnO could be significantly enhanced by Ni doping, which is due to increase the visible light absorption of the catalyst and decrease the recombination of the photo generated charge carriers. Further, the biosynthesized Ni doped ZnO NPs using aloe vera leaf extract have proved themselves tobe an effective antibacterial agent against E.Coli, Klbsiella Pneumoniae, Staphylococcus aureus, and Streptococcus pyogenes. Hence it could be considered as a non-hazardous, eco-friendly method for the synthesis and future applications in the field of waste water treatment and biological applications.

References

[1]TongH, O., & BiY, P, Advanced Materials, 24(2), 229(2012); https://doi.org/10.1002/adma.201102752

[2] D. North and R. Thomas, "How the West Grew Rich: The Economic Transformation of the Industrial World, New York", Basic Books (1986).

[3] Robinson, T., McMullan, G., Marchant, R., Nigam, P., Bioresource technology 77(3), 247(2001); https://doi.org/10.1016/S0960-8524(00)00080-8

[4]. Sboui, M., Bouattour, S., Gruttadauria, M., Marcì, G., Liotta, L. F., Boufi, S, Nanomaterials, 10(3), 470 (2020); https://doi.org/10.3390/nano10030470

[5]. Li, S., Xue, B., Wu, G., Liu, Y., Zhang, H., Ma, D., Zuo, J. Nanomaterials, 9(11), 1562(2019); https://doi.org/10.3390/nano9111562

[6]Hanley, C., Layne, J., Punnoose, A., Reddy, K., Coombs, I., Coombs, A., Wingett, D. Nanotechnology, 19(29), 295103(2008); https://doi.org/10.1088/0957-4484/19/29/295103

[7] Nie, S., Xing, Y., Kim, G. J., Simons, J. W, Annu. Rev. Biomed. Eng., 9, 257(2007); https://doi.org/10.1146/annurev.bioeng.9.060906.152025

[8] Boomi, P., Poorani, G. P., Palanisamy, S., Selvam, S., Ramanathan, G., Ravikumar, S., Saravanan, M. Journal of Cluster Science, 30(3), 715(2019); https://doi.org/10.1007/s10876-019-01530-x

[9] Hu, X., Cook, S., Wang, P., & Hwang, H. M., Science of the Total Environment, 407(8), 3070(2009); https://doi.org/10.1016/j.scitotenv.2009.01.033

[10] Kołodziejczak-Radzimska, A., Jesionowski, T. Materials 7, 2833(2014); https://doi.org/10.3390/ma7042833

[11] Zhang, Z. Y., Xiong, H. M. Materials, 8(6), 3101(2015); https://doi.org/10.3390/ma8063101

[12] Kim, S., Lee, S. Y., Cho, H. J. Nanomaterials, 7(11), 354(2017); https://doi.org/10.3390/nano7110354

[13] Fouda, A., EL-Din-Hassan, S., Salem, S. S., Shaheen, T, Microb. Pathog. 125, 252 (2018); https://doi.org/10.1016/j.micpath.2018.09.030

[14] Liu, J., Kang, Y., Yin, S., Song, B., Wei, L., Chen, L., Shao, L. International journal of nanomedicine, 12, 8085(2017); https://doi.org/10.2147/IJN.S149070

[15] Fouda, A., Saad, E. L., Salem, S. S., &Shaheen, T. I. Microbial pathogenesis 125, 252(2018); https://doi.org/10.1016/j.micpath.2018.09.030

[16] Agarwal, H., Menon, S., Kumar, S. V., Rajeshkumar, S. Chemico-biological interactions, 286, 60(2018); https://doi.org/10.1016/j.cbi.2018.03.008

[17] Kiranmai, M., Kadimcharla, K., Keesara, N. R., Fatima, S. N., Bommena, P., Batchu, U. R. Indian Journal of Pharmaceutical Sciences, 79(5), 695(2017).

[18] Taherian, S. M. R., Hosseini, S. A., Jafari, A., Etminan, A. Herbal Medicines Journal, 3(4), 147(2019).

[19] Zare, E., Pourseyedi, S., Khatami, M., Darezereshki, E. Journal of Molecular Structure, 1146, 96(2017); https://doi.org/10.1016/j.molstruc.2017.05.118

[20] Bala, N., Saha, S., Chakraborty, M., Maiti, M., Das, S., Basu, R., Nandy, P. RSC Advances, 5(7), 4993(2015); https://doi.org/10.1039/C4RA12784F

[21] Karthik, S., Siva, P., Balu, K. S., Suriyaprabha, R., Rajendran, V., Maaza, M. Advanced Powder Technology, 28(12), 3184(2017); https://doi.org/10.1016/j.apt.2017.09.033

[22] Mahendra, C., Murali, M., Manasa, G., Ponnamma, P., Abhilash, M. R., Lakshmeesha, T. R., Sudarshana, M. S. Microbial pathogenesis, 110, 620(2017); https://doi.org/10.1016/j.micpath.2017.07.051

[23] Raja, A., Ashokkumar, S., Marthandam, R. P., Jayachandiran, J., Khatiwada, C. P., Kaviyarasu, K., Swaminathan, M , Journal of Photochemistry and Photobiology B: Biology, 181, 53(2018); https://doi.org/10.1016/j.jphotobiol.2018.02.011

[24] Pavithra, N. S., Lingaraju, K., Raghu, G. K., Nagaraju, G. Spectrochimica Acta Part A: Molecular and Biomolecular Spectroscopy, 185, 11(2017); https://doi.org/10.1016/j.saa.2017.05.032

[25] Radha, M. H., &Laxmipriya, N. P, Journal of traditional and complementary medicine, 5(1), 21(2015); https://doi.org/10.1016/j.jtcme.2014.10.006

[26] Mendy, T. K., Misran, A., Mahmud, T. M. M., Ismail, S. I., Scientia Horticulturae, 257, 108767(2019); https://doi.org/10.1016/j.scienta.2019.108767

[27] Venkataraju, J. L., Sharath, R., Chandraprabha, M. N., Neelufar, E., Hazra, A., Patra, M. Journal of Biochemical Technology, 3(5), 151(2014).

[28] Shi, W. G., Liu, W., Yu, W., Zhang, Y., Ding, S., Li, H., Luo, Z. B. Journal of hazardous materials, 362, 275(2019); https://doi.org/10.1016/j.jhazmat.2018.09.024

[29] Khoshhesab, Z. M., Sarfaraz, M., Asadabad, M. A.,Metal-Organic, and Nano-Metal Chemistry, 41(7), 814(2011); https://doi.org/10.1080/15533174.2011.591308

[30] Sivakarthik, P., Thangaraj, V., Parthibavarman, M. Journal of Materials Science: Materials in Electronics, 28(8), 5990(2017); https://doi.org/10.1007/s10854-016-6274-7

[31] Cullity, B. D. Elements of X-Ray Diffraction, Addition-Wesley Co. Readings, MA, 102(1978).

[32] Peng, Y. Z., Liew, T., Song, W. D., An, C. W., Teo, K. L., Chong, T. C. Journal of superconductivity, 18(1), 97(2005); https://doi.org/10.1007/s10948-005-2158-4

[33] Moss, T. S., The interpretation of the properties of indium antimonide. Proceedings of the Physical Society. Section B, 67(10), 775(1954); https://doi.org/10.1088/0370-1301/67/10/306

[34] Misra, M., Kapur, P., Nayak, M. K., Singla, M., New Journal of Chemistry, 38(9), 4197(2014); https://doi.org/10.1039/C4NJ00569D

[35] Zhou, J., Zhang, M., Zhu, Y., Physical Chemistry Chemical Physics, 16(33), 17627(2014); https://doi.org/10.1039/C4CP02061H

[36] Yuvakkumar, R., Suresh, J., Saravanakumar, B., Nathanael, A. J., Hong, S. I., Rajendran, V. Spectrochimica Acta Part A: Molecular and Biomolecular Spectroscopy, 137, 250(2015); https://doi.org/10.1016/j.saa.2014.08.022

[37] Das, D., Nath, B. C., Phukon, P., &Dolui, S. K., Colloids and Surfaces B: Biointerfaces, 101, 430(2013); https://doi.org/10.1016/j.colsurfb.2012.07.002

[38] Durairasan, M., Karthik, P. S., Balaji, J., &Rajeshkanna, B., Diamond and Related Materials, 111, 108174(2021); https://doi.org/10.1016/j.diamond.2020.108174

[39] SivaKarthik, P., Thangaraj, V., Kumaresan, S., Vallalperuman, K. Journal of Materials Science: Materials in Electronics, 28(14), 10582(2017); https://doi.org/10.1007/s10854-017-6832-7

[40] Sivakarthik, P., Thangaraj, V., Perumalraj, K., Balaji, J., Digest Journal of Nanomaterials and Biostructures, 11(3), 935(2016).

[41] Pan, L., Liu, X., Sun, Z., Sun, C. Q., Journal of materials chemistry A, 1(29), 8299(2013); https://doi.org/10.1039/c3ta10981j

[42] Soren, S., Kumar, S., Mishra, S., Jena, P. K., Verma, S. K., Parhi, P., Microbial Pathogenesis, 119, 145(2018); https://doi.org/10.1016/j.micpath.2018.03.048

[43] Soren, S., Kumar, S., Mishra, S., Jena, P. K., Verma, S. K., Parhi, P., Microbial Pathogenesis, 119, 145(2018); https://doi.org/10.1016/j.micpath.2018.03.048

[44] Raghupathi, K. R., Koodali, R. T., Manna, A. C., Langmuir, 27(7), 4020(2011); https://doi.org/10.1021/la104825u

[45] Dadi, R., Azouani, R., Traore, M., Mielcarek, C., Kanaev, A. Materials Science and Engineering: C, 104, 109968(2019); https://doi.org/10.1016/j.msec.2019.109968